PCCP

Accepted Manuscript

This is an *Accepted Manuscript*, which has been through the Royal Society of Chemistry peer review process and has been accepted for publication.

Accepted Manuscripts are published online shortly after acceptance, before technical editing, formatting and proof reading. Using this free service, authors can make their results available to the community, in citable form, before we publish the edited article. We will replace this *Accepted Manuscript* with the edited and formatted *Advance Article* as soon as it is available.

You can find more information about *Accepted Manuscripts* in the **Information for Authors**.

Please note that technical editing may introduce minor changes to the text and/or graphics, which may alter content. The journal's standard **Terms & Conditions** and the **Ethical guidelines** still apply. In no event shall the Royal Society of Chemistry be held responsible for any errors or omissions in this *Accepted Manuscript* or any consequences arising from the use of any information it contains.

Journal Name

COMMUNICATION

Retarded Dopant Diffusion by Moderated Dopant-Dopant Interactions in Si Nanowires

Jongseob Kim[a] and Ki-Ha Hong[*b]

The retarded dopant diffusion in Si nanostructures is investigated using the first principles calculation. It is presented that weak dopant-dopant interaction energy (DDIE) in nanostructures is responsible for the suppressed dopant diffusion in comparison with that in bulk Si. The DDIE is significantly reduced as the diameter of Si nanowire becomes smaller. The mechanical softening and quantum confinement found in nanostructures are the physical origin for the small interaction energy. Reduced dopant-dopant interaction slows down the diffusion process from heavily doped region to undoped regions. Thus, we suggest that additional annealing process is indispensable to make desired dopant profile in the nanoscale semiconductor devices.

Nanotechnology has enabled the fabrication of various electrical devices based on nanoscale materials such as quantum dots and nanowires. Doping is one of the key processes to modulate the electrical properties of the constituent materials. However, there have been reports on the fundamental difficulties involved in the doping of nano-materials.[1-3] To explain the origin of the difficulties in nanoscale doping, theories on the physical mechanism of dopants characteristics in nanostructures have been developed to reveal various unique characteristics of dopants behaviors in nanomaterials.[4-6]

Uniform dopant distribution in nanostructures is commonly preferred and diffusion is an essential process to make engineered dopant profiles. However, the diffusion in the nanostructures shows unusual behaviors[7] and dopant segregation in nanowires,[8] which cannot be understood in the context of bulk diffusion. To address the dopant diffusion in semiconductor nanowires, experimental studies have been made on non-uniform radial dopant distribution profiles, which required an additional annealing process to obtain uniform dopant distribution.[9,10]

Dopant diffusion is commonly accompanied by the nanowire growth and the diffusion profiles can be significantly affected by growth process conditions.[11] This makes it difficult to isolate the diffusion phenomena from other process dependent artifacts. Xie et al.'s controlled experiments on dopant diffusion behaviors in Si and Ge nanowires is worth to notice in that they reported diameter dependent dopant location in nanowires where the diffusion process is decoupled with growth step.[8] They showed that the dopants hardly penetrate from surface to center region when their diameters are less than 20 nm. Such reduced diffusion in nanostructures could not be explained with either the self purification[4] or the dielectric confinement[5].

These recent experimental reports instigate a theoretical investigation on the fundamental mechanism for the suppressed dopant diffusion in nanostructures. To understand the atomic behaviors in diffusion from the aforementioned experiments, the first principles calculation analysis can be useful for isolating the effects of a single parameter while excluding various perturbations in real systems.[12-17] Although there have been previous ab initio studies on the size and position dependence of a single dopant and co-dopants formations in silicon nanostructures[18-20], the multiple dopants contribution on the system energy of nano-structures has not been addressed.

In this study, we report the origin of suppressed dopant diffusion in SiNWs through the first principles calculation on the formation energy of multi-dopant nanostructures. Although there was a previous trial to estimate the dopant-dopant interaction in large SiNWs,[21] they did not consider the undoped SiNWs as the reference material to dope. Neglecting the energy of pure SiNWs cannot reflect the system energy changes induced by the quantum confinement and surface stress according to the diameter variation. Instead, we adopt the pure silicon nanowires as the reference materials in the formation energy calculations in accordance with the previous successful studies[6,18-20,22] and focused on finding the basic mechanism of the dopant-dopant interaction changes in nanostructures. Our results show that the dopant-dopant interaction is significantly reduced in nanostructures, which makes the dopant diffusion slower, resulting in a non-uniform distribution in the SiNWs as have been observed experimentally.
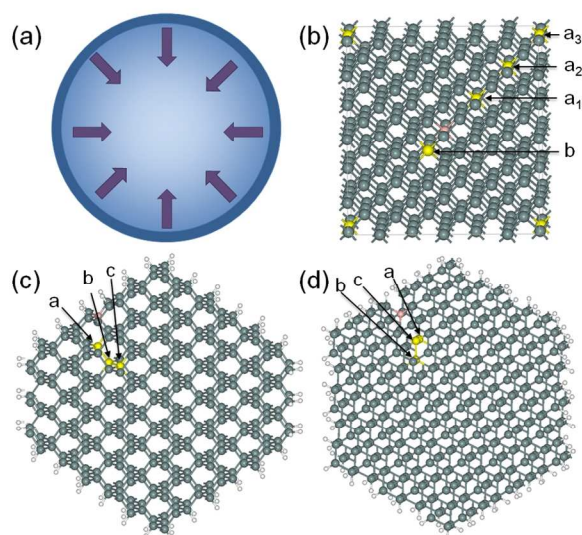
Fig. 1. (a) Schematic diagram of modeled dopant diffusion process in this calculation study. (b) Atomic configuration of dopants in bulk supercell. Pink ball represents the first reference B site and yellow balls represent the location of second B. a_1~a_3 sites are along [111] direction and the distance between nearest B atoms is 3.685 Å before geometry optimization. The distance between reference B and b sites is 4.517 Å. Atomic structures of (c) [110] and (d) [111] SiNWs of which diameter is about 3.1 nm. [110] and [111] SiNWs consist of 72 H and 288 Si+B and 90 H and 338 Si+B atoms, respectively.

To obtain formation energies of dopants in SiNWs, we perform density functional theory (DFT) calculations using the VASP program package.[23,24] Plane wave basis expansions with an energy cutoff of 350 eV and the generalized gradient approximation (GGA) with PBE exchange-correlation functional are used. The core-valence interaction is described by the projector-augmented wave (PAW) method.[25] Atomic positions are optimized until the residual forces on each atom are less than 0.01 eV/Å. Silicon supercell containing 216 atoms is used for the estimation of bulk properties. [110] and [111] directional SiNWs with diameters up to 3.2 nm are considered and surfaces are passivated with hydrogen. We apply Monkhorst-Pack sampling for the supercell with a $2 \times 2 \times 2$ k-point grid. For the nanowires, $1 \times 1 \times m$ k-point sampling is selected in which m is even number and excluded Γ-point[26] (m

is set to 4 and 2 for the [110] and [111] nanowires, respectively). To reduce the cell to cell interaction, the distance between neighboring wires set to be longer than 10 Å.

Dopants tend to diffuse from highly concentrated surface region to the low concentrated core regions in SiNWs as depicted in schematic diagram, Fig. 1a.[8] High doping concentration in the nanowire surface region induces high chemical potential which makes the dopants diffuse from the surface into the core of SiNWs.[7] We calculate the formation energy variation by changing the distance between two dopants where boron atom (B) is selected as the dopant. Fig. 1b~1d show the atomic configurations used in this study for the bulk supercell, [110] and [111] SiNWs, respectively. The doping concentrations in our calculations with one B are 2.3×10^{20}/cm^3, 1.7×10^{20}/cm^3 and 1.5×10^{20}/cm^3 for the bulk supercell, [110] SiNW and [111] SiNWs respectively, which corresponds to the doping concentration of the nanowire surface during growth procedure up to the order of magnitude.[7] To exclude the effects of the periodic boundary condition, the axial length of nanowire supercell should be carefully chosen. We check the formation energy change when one boron is located at the center of the 2.5 nm [110] SiNW by varying the number of axial unitcell and the result is described in the Fig. S1 (ESI†). The axial unitcell length of [110] SiNW is 3.87 Å and the 2 unit cell is large enough to neglect the effects of the periodic boundary condition as shown in previous report[21]. Thus we selected 2 unitcell along axial direction for the [110] SiNWs. As the unit axial length of [111] SiNW is 9.47 Å, one unitcell along axial direction is enough for the formation energy calculation.

The repulsive interaction energy between dopants including Coulomb force causes the dopants to diffuse. The interaction energy between dopants can be estimated by the computation of energy changes between multi-dopants system and single-dopant system. There are two criteria for the selection of multi-dopant configurations. First, boron-pair sites are avoided since it is well known that dopant pairs lose the role of carrier generators and moreover acceptor pairs are not energetically favored.[27] Second, surface Si sites are not chosen since the dopants at the surface Si sites prefer to make dangling bonds, losing the dopant characteristics.[6,19,28] In the bulk supercell, we place the first B (pink ball in the Fig. 1b) at the center and place a second B not to form a boron-pair (the nearest distance between two boron dopants is 3.685 Å). For Si nanowires, the first B site is chosen at the subsurface Si (pink ball in the Fig 1c and 1d) as the reference site to assimilate the diffusion process. Fig. 2a represents the formation energy variation while
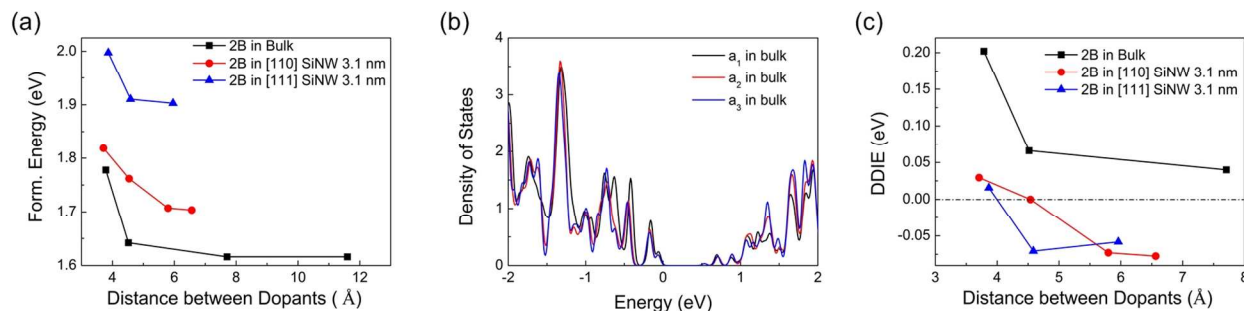

Fig. 2. (a) Dopant formation energy in the bulk, [110] and [111] SiNWs with varying the distance between 2 boron dopants. (b) Density of states of the bulk supercell with 2 boron dopants when first boron is at reference site (pink ball in Figure 1) and second boron is at a_1/a_2/a_3 site in Figure 1b. (c) Dopant-dopant interaction energy (DDIE) of dual boron with respect to the inter-dopant distance. Interaction energy is defined by the energy difference between the formation energy including 2 boron in the cell and the sum of formation energies when the single B is individually located at each positions.

changing the distance between dopants in the bulk Si and [110] and [111] SiNWs of which diameter is 3.2 nm. Formation energies (E_f) are calculated as follows,

$$E_f = E(\text{B doped SiNW}) - E(\text{SiNW}) + n\,(\mu_{Si} - \mu_B)$$

where E(B doped SiNW) and E(SiNW) are the total energy of the SiNW with and without B dopants, respectively. J AndJ μ_{Si} and μ_B are the chemical potential of Si and B obtained from the bulk energy calculation and n is the number of B dopants in SiNW. We use the total energy per atom in the tetragonal B_{50} crystal for the μ_B. In this definition, the positive formation energy means less stable. The dopant-dopant interaction energy (DDIE) of this study is defined as the energy difference between the formation energy when the 2 dopants exists simultaneously and the summation of formation energies when each Boron exists individually which can be given by,

$$\text{DDIE} = E_f(B_1 + B_2) - E_f(B_1) - E_f(B_2)$$

In this definition, the positive DDIE means the rise of total energy and strong DDIE represents the repulsive energy gain between near dopants. As the formation energy (E_f) of single B in the supercell is 0.79 eV, the formation energy of two B in the cell is expected to be 1.58 eV in the absence of dopant-dopant interaction.

The formation energy of two borons in bulk supercell, shown in Fig. 2a, converges fast to 1.62 eV. The density of states (DOS) of bulk calculations in Fig. 2b shows the negligible dopant-dopant interaction when the distance between dopants is longer than 6 Å. In Si nanowires, the convergence of formation energy near 6 Å is similar with the bulk Si. However, there are two notable differences. The first is the overall increase of the formation energy which can be ascribed to the nanostructure itself. The second is the decrease of the energy difference between the nearest and the saturation point in nanowires. Since the formation energy at saturation level is approximately the sum of the formation energy of two individual dopants, the energy difference between the nearest and the saturation point would indicate the DDIE itself. We can therefore surmise from Fig. 2a that the DDIE has decreased for the case of nanowires. The charge density profile of valence band maximum of the nearest 2 B case (B is at a1 in Fig. 1b) shows different correlation with that of the farthest 2 B case (B is at a3 in Fig. 1b) that are presented in Fig. S3 (ESI†).

To see this more clearly, Fig. 2c shows the dopant-dopant interaction energy when 2 borons are at B (reference site shown as a pink ball in the Fig. 1) and B' sites (one of yellow sites in the Fig. 1). For the bulk calculation, the interaction energy between 2 B is 200 meV for the nearest case. For nanowires with diameter 3.1 nm, this interaction energy decreases to be 29 meV and 16 meV for [110] and [111] SiNW, respectively. As the distance between dopants becomes apart, the interaction energy in the Si bulk decreases to under 50 meV. The interaction energies for nanowires even show negative value when the distance between 2B is longer than 4.5 Å. This represents that the energy increase from the dopant segregation becomes negligible for the nanowires and the dopant diffusion is hardly accelerated by the existence of a nearby dopant.

There are two plausible origins for this reduction of repulsive interaction energy between dopants in nanostructures. One is the geometrical relaxation and the other is the weakened interaction induced by the change in the band gap, the quantum

confinement effect. Geometry relaxation factors are assessed by calculating the energy difference between relaxed and frozen atom structures, *i.e.* the calculation of the energy when the positions of atoms are fixed. Geometry relaxation energy when the inter-Boron distance is smallest is represented in the black square in Fig. 3a. Comparing with the formation energy of the relaxed structure (Fig. 2a), it shows that the main contribution to energy minimization originates from this geometry relaxation. The relaxation energy for the nanowires is larger than that of bulk case by at least 200 meV. And Figure 3a shows that the contribution of geometry relaxation energy of [111] SiNW is higher than that of [110] NW. As the diameter shrinks, the mechanical properties become more vulnerable to surface stress, which results in the softening of SiNWs. Leu et al.[29] showed that the Young's modulus becomes smaller as the diameter of SiNWs gets smaller and moreover the softening of [111] SiNWs is more significant than that of [110] SiNWs due to the large surface elasticity moduli of {110} surfaces, which envelop the surfaces of [111] directional NWs.
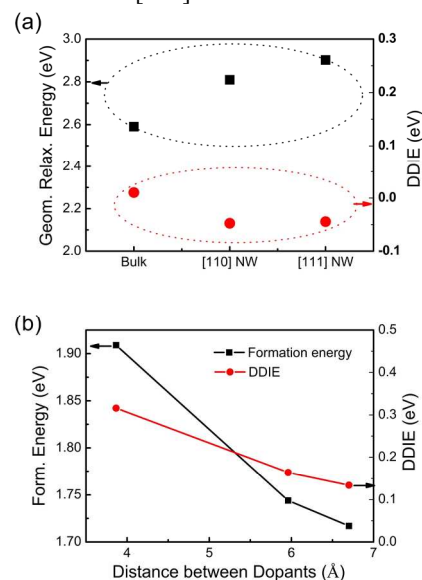

Fig. 3. (a) Geometry relaxation energy (left y) and DDIE (right y) of Si bulk and [110] and [111] SiNWs with smallest inter-boron distance. (b) Formation energy (left y) and dopant-dopant interaction energy (right y) variations with respect to dopant-dopant distances in Si slab.

Table 1. DDIE in [110] SiNW with multi-Boron dopants when the diameters are changed. Cen and SS represent the center of the NW and sub-surface location respectively. Cen-Cen is the case when the 2 B are located at the center and SS-SS-SS is when the 3 B locate at sub-surface of NW. The atomic configurations are described in Fig. S2 (ESI†). (energy is in meV)

Diameter	2.5nm	3.1nm	3.8nm
Cen-Cen	85	137	156
SS-SS	36	64	111
SS-SS-SS		95	193

The other factor to be considered is the weakened interaction between dopants induced by the quantum confinement. As the

size of nanowires shrinks, the band gap increases and the dielectric constant becomes smaller. This results in the reduced effective Bohr radius for the dopant in the nanostructure, which suppresses the interaction between dopants and more confines the charge density of the valence band induced by B incorporation. The charge densities in bulk and silicon nanowire are compared in Fig. 4.

The red circles in Fig. 3a represent the DDIE for the frozen atom structures. For the nanowires, negative interaction energies about 45 meV are observed, which shows that there can be energy gain for the NWs to have the dopant segregation even without geometry relaxation effects. As the actual electronic interaction between dopants can be changed for the relaxed structure, we calculate the DDIE for the [110] SiNWs by changing diameters. Following Leu et al., the change in Young's modulus for the [110] SiNWs is less than 10 % when the diameter changes from 1 nm to 2.6 nm and approaches the bulk Young's modulus above 2.6 nm, in which case the geometrical contribution to the DDIE is minimal. Thus we can estimate the electronic interaction energy contribution by observing the DDIE changes with the diameter of SiNWs.

Table 1 represents the interaction energies for the various configurations when the diameter of [110] SiNWs is between 2.5 nm and 3.8 nm. As the diameter becomes smaller, the interaction energy consistently decreases for all considered configurations. The DDIE at the center (Cen) is stronger than that at the sub-surface (SS). For both Cen-Cen and SS-SS configurations, the DDIE decreases by about 70 meV, which can be considered as coming from the reduced electronic interaction due to the quantum confinement effect.

In order to validate our conjecture, suppressed dopant diffusion in nanostructured materials, we have calculated the DDIE for the surface structure. The reduced formation energy even for the surface structure will also appear if the independent dopant formation energy for the multi dopants in nanostructures comes from the surface effects only. The considered atomic slab structure is depicted in Fig. S3 (ESI†). Fig. 3b shows that the formation energy induced by sub-surface Boron and its nearest Boron (except di-Boron pair) is 1.91 eV and the DDIE is 320 meV. This shows that only surface stress effects cannot make the reduced dopant correlation.

It is well known that GGA-PBE calculations underestimate the band gap as shown in Figure 2b. Rurali et al.[30] presented that the ionization energies of donor derived by hybrid functional calculations are deeper than those obtained with stand density functional theory. Thus we believe that the reduced dopant interaction for nanowires might not be affected by applying hybrid density functionals. Quantitative analysis may need the exact evaluation of the dopant energy levels using advanced density functional theory such as hybrid methods[31,32] calculation.

We have analyzed the reduction in DDIE both from the perspective of mechanical softening and electronic interaction. Both mechanisms lead to the reduction in DDIE which implies lower diffusivity of dopants in nanowires, in accordance with experimental results. Furthermore, understanding the underlying mechanism enables us to make relative predictions about the doping characteristics of different Si nanowires from their mechanical and bandgap properties, to help facilitate the fabrication of nano devices.
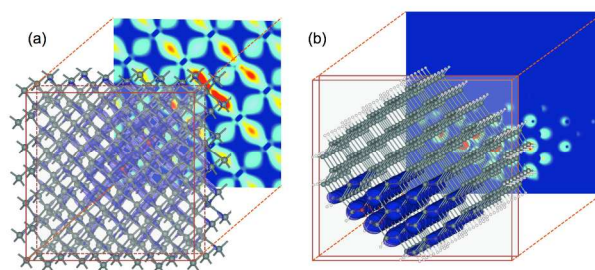

Fig. 4. Charge density profiles for (a) 2 B in Silicon supercell and (b) 2B in 2.5 nm diameter Si nanowire per unit cell.

Conclusions

The reduced dopant diffusion in the SiNWs has been investigated using density functional theory. Our result revealed that the DDIE between nearby dopants is significantly reduced as the diameter of SiNWs becomes smaller. The origin of reduced DDIE can be explained with the mechanical softening and the quantum confinement generated in the SiNWs. The reduced DDIE in Si nanostructures suppresses the dopant diffusion from heavily doped region into undoped region. Therefore, longer diffusion process time is necessary to generate optimal dopant profile in the nano-scale semiconductor devices. Especially, when the nanowire growth direction is selected to be mechanically softer direction or have strongly quantum confined cross-section, the effect would be intensified. For the SiNWs, [111] SiNWs needs more diffusion time than [110] SiNWs for the same diameter.

Although the diffusion in nanostructures are affected by various factors such as surface passivation, temperature, pressure, and other process variables, our theoretical prediction of the dopant behaviors in the nanostructures can serve as a fundamental understanding why nanoscale diffusion is different from the bulk behavior and how to control the diffusion process to make uniform dopant profile.

Acknowledgements

Notes and references

a Samsung Advanced Institute of Technology, Samsung Electronics Co., Ltd. Mt. 14-1, Nongseo-Dong, Giheung-Gu, Yongin-Si, Gyeonggi-Do 446-712, Korea. E-mail: jongs.kim@samsung.com
b Department of Materials Science and Engineering, Hanbat National University, 125 Dongseo-daero, Yuseong-Gu, Daejeon, 305-719 Korea. E-mail: kiha.hong@hanbat.ac.kr

1. D. J. Norris, A. L. Efros, and S. C. Erwin, *Science*, 2008, **319**, 1776–1779.

2. M. T. Björk, H. Schmid, J. Knoch, H. Riel, and W. Riess, *Nature Nanotech.*, 2009, **4**, 103–107.
3. X. Ou, N. Geyer, R. Kögler, P. Werner, and W. Skorupa, *Appl. Phys. Lett.*, 2011, **98**, –.
4. G. Dalpian and J. Chelikowsky, *Phys. Rev. Lett.*, 2006, **96**, 226802.
5. M. Diarra, Y.-M. Niquet, C. Delerue, and G. Allan, *Phys. Rev. B*, 2007, **75**, 045301.
6. K.-H. Hong, J. Kim, J. H. Lee, J. Shin, and U.-I. Chung, *Nano Lett.*, 2010, **10**, 1671–1676.
7. V. C. Holmberg, M. G. Panthani, and B. A. Korgel, *Science*, 2009, **326**, 405–407.
8. P. Xie, Y. Hu, Y. Fang, J. Huang, and C. M. Lieber, *Proc. Natl. Acad. Sci. U.S.A.*, 2009, **106**, 15254–15258.
9. D. E. Perea, E. R. Hemesath, E. J. Schwalbach, J. L. Lensch-Falk, P. W. Voorhees, and L. J. Lauhon, *Nature Nanotech.*, 2009, **4**, 315–319.
10. E. Koren, J. K. Hyun, U. Givan, E. R. Hemesath, L. J. Lauhon, and Y. Rosenwaks, *Nano Lett.*, 2011, **11**, 183–187.
11. J. G. Connell, K. Yoon, D. E. Perea, E. J. Schwalbach, P. W. Voorhees, and L. J. Lauhon, *Nano Lett.*, 2013, **13**, 199–206.
12. M. A. Sk, M.-F. Ng, L. Huang, and K. H. Lim, *Phys. Chem. Chem. Phys.*, 2013, **15**, 5927–5935.
13. N. Gao, W. T. Zheng, and Q. Jiang, *Phys. Chem. Chem. Phys.*, 2011, **14**, 257–261.
14. J.-H. Lee, *Phys. Chem. Chem. Phys.*, 2014, **16**, 2425–2429.
15. K.-H. Hong, J. Kim, S.-H. Lee, and J. K. Shin, *Nano Lett.*, 2008, **8**, 1335–1340.
16. J. Kim, J. H. Lee, and K.-H. Hong, *J. Phys. Chem. Lett.*, 2013, **4**, 121–126.
17. P. W. Leu, B. Shan, and K. Cho, *Phys. Rev. B*, 2006, **73**, 195320.
18. H. Peelaers, B. Partoens, and F. M. Peeters, *Nano Lett.*, 2006, **6**, 2781–2784.
19. M. V. Fernández-Serra, C. Adessi, and X. Blase, *Nano Lett.*, 2006, **6**, 2674–2678.
20. C. R. Leao, A. Fazzio, and A. J. R. da Silva, *Nano Lett.*, 2008, **8**, 1866–1871.
21. M.-F. Ng, M. B. Sullivan, S. W. Tong, and P. Wu, *Nano Lett.*, 2011, **11**, 4794–4799.
22. J. Kim, K. Y. Kim, H. J. Choi, and K.-H. Hong, *J. Phys. Chem. C*, 2014, **118**, 20710–20715.
23. G. Kresse and J. Hafner, *Phys. Rev. B*, 1993, **47**, 558.
24. G. Kresse and J. Furthmüller, *Comput. Mater. Sci.*, 1996, **6**, 15–50.
25. P. E. Blöchl, *Phys. Rev. B*, 1994, **50**, 17953–17979.
26. C. G. Van de Walle, *J. Appl. Phys.*, 2004, **95**, 3851.
27. C.-Y. Moon, W.-J. Lee, and K. J. Chang, *Nano Lett.*, 2008, **8**, 3086–3091.
28. A. K. Singh, V. Kumar, R. Note, and Y. Kawazoe, *Nano Lett.*, 2006, **6**, 920–925.
29. P. W. Leu, A. Svizhenko, and K. Cho, *Phys. Rev. B*, 2008, **77**, 235305.
30. R. Rurali, B. Aradi, T. Frauenheim, and Á. Gali, *Phys. Rev. B*, 2009, **79**, 115303.
31. B. G. Janesko, *J. Chem. Phys.*, 2011, **134**, 184105.
32. B. M. Wong and J. G. Cordaro, *J. Phys. Chem. C*, 2011, **115**, 18333–18341.

Physical Chemistry Chemical Physics Accepted Manuscript